

M. J. Henze · F. Schaeffel · M. Ott

## Variations in the off-axis refractive state in the eye of the Vietnamese leaf turtle (*Geoemyda spengleri*)

Received: 28 July 2003 / Revised: 27 October 2003 / Accepted: 8 November 2003 / Published online: 10 December 2003  
© Springer-Verlag 2003

**Abstract** Lower-field myopia has been described for various vertebrates as an adaptation that permits the animal to keep the ground in focus during foraging, and, at the same time, to look out for distant objects, such as predators, in the upper visual field. Off-axis measurements with infrared photoretinoscopy in the eye of *Geoemyda spengleri* revealed a constant refractive state in the horizontal plane of the visual field but variable refraction in the vertical plane. In the three turtles investigated, the refractions increased continuously from the ventral to the dorsal visual field over a range of 35, 40 and 56 D, respectively. While this finding confirms the presence of an adaptive change of the refractive state equivalent to lower field myopia, subsequent measurements with a rotated retinoscope showed that at least part of the variation in the ventral field was attributed to astigmatism. The reason for this astigmatism is unknown. Anatomical investigation of the retina revealed that the constant refractive values in the horizontal plane corresponded to a stripe of increased ganglion cell density. A maximum density of 4,200 ganglion cells  $\text{mm}^{-2}$  was counted in the centre of this visual streak.

**Keywords** Astigmatism · Infrared photoretinoscopy · Lower-field myopia · Ramp retina · Visual streak

### Introduction

Vertebrates that live on or near to the ground usually see the lower part of their visual field closer than portions in the middle or upper field of view. Because of this variation of distances, large parts of the retinal image are out of focus at a given refractive state of the eye. Lower-field myopia is an adaptation that keeps the ground plane in focus while the animal is looking at distant objects in its middle and upper visual field. The presence of lower-field myopia has been demonstrated for several ground-foraging species, namely for pigeons (Catania 1964; Millodot and Blough 1971; Nye 1973; Fitzke et al. 1985), quails, cranes (Hodos and Erichsen 1990), chickens (Hodos and Erichsen 1990; Schaeffel et al. 1994) and frogs and toads (Schaeffel et al. 1994). It is not known which mechanism accounts for the observed changes in the refractive state. As a possible explanation, ramp retinas have been described for horses and rays (Walls 1942), with the upper part of the retina more distant from the nodal point of the eye than the lower part. However, the significance of this ocular asymmetry has been questioned (Sivak 1976).

In the study reported here, the refractive state in the eye of Vietnamese leaf turtles (*Geoemyda spengleri*) was measured both along the optical axis and off-axis. In a related paper (Henze et al. 2004), a highly precise accommodative response was observed in *G. spengleri*, which indicated excellent vision. Because Vietnamese leaf turtles forage on the ground, adaptations to compensate for the different focal distances in the upper and lower visual field can be expected. We quantified off-axis refraction in both the horizontal and vertical plane of the visual field using the technique of infrared photoretinoscopy. Astigmatism as a source of refractive state variation was considered by measuring the refraction both in the vertical and horizontal ocular meridian (Schaeffel et al. 1994). By anatomical investigation of the retina, the density of ganglion cells was counted in order

M. J. Henze · M. Ott (✉)  
Institute for Anatomy, University of Tübingen,  
Österbergstraße 3, 72074 Tübingen, Germany  
E-mail: ott@anatu.uni-tuebingen.de  
Tel.: +49-7071-2973026  
Fax: +49-7071-294014

F. Schaeffel  
Section of Neurobiology of the Eye, Department II,  
University Eye Hospital, Calwerstr. 7/1,  
72076 Tübingen, Germany

to correlate the variation of the refractive state with areas of putative high visual resolution.

## Materials and methods

### Animals

Eleven adult Vietnamese leaf turtles were obtained from a commercial supplier. They were kept in a terrarium under a 12 h/12 h light/dark-cycle. The air temperature changed between 19°C at night and 26°C by day. Humidity was maintained at high levels by using a moist substrate and spraying the furnishings regularly with water. The animals were fed on insect larvae, earthworms and neonate mice.

### Refractive measurements

To determine the refractive state of the eye, we used infrared photoretinoscopy as described in detail by Schaeffel et al. (1987, 1994). This technique is well suited to study alert, unrestrained animals since it does not disturb them. Our photoretinoscope (Fig. 1) consisted of 13 infrared light-emitting diodes (IR-LEDs) positioned on a shield in front of the lower part of the aperture of an infrared sensitive video camera (Canon CI-20 PR equipped with a Zeiss  $f/1.4$ , 85-mm lens). The LEDs were arranged in 4 horizontal rows at different distances (eccentricities) from the optical axis of the camera and operated simultaneously. The IR-light from the LEDs was partly reflected by the ocular fundus and caused a vertical brightness profile in the pupil. The slope of this intensity

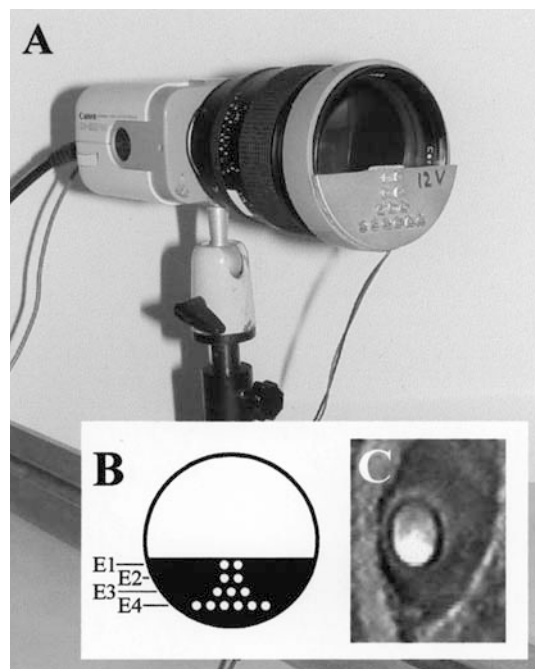


**Fig. 1A–C** Equipment for the measurements of the refractive state of the eye. An infrared (IR) photoretinoscope was placed in front of the lens aperture of an IR-sensitive video camera (A). It consisted of 13 IR light-emitting diodes (IR-LEDs) arranged in 4 parallel rows at different eccentricities (E1–E4). They were fixed to a shield that covers slightly less than half of the lens aperture (B). This arrangement induced an intensity profile of the light reflex from the ocular fundus (C). In the example shown here, the light reflex is clearly visible in the lower part of the pupil. This indicates active accommodation. In the remaining figures, measurements of refractive state variation in the visual field are shown for the relaxed, non-accommodated eye

profile (Fig. 1C) changes linearly with the refractive state of the eye (Schaeffel et al. 1994) and can be calibrated individually by placing ophthalmic lenses of different refractive power in front of the cornea (see Henze et al. 2004 for details).

Refractions were done under a reduced ambient light level (30–50 lx) at the relaxed, non-accommodating eye. Refractions that include spontaneous accommodation were excluded from the database. This was a prerequisite to examine variations of the refractive state over the visual field. The camera was moved on a circular path in front of the eye (radius = 70 cm) along the vertical and the horizontal plane bisecting it. The refractive state was recorded continuously and later correlated with the corresponding visual angle. This angle was calculated from the position of the first (=corneal) Purkinje reflex of the IR-LEDs. We assumed that the optical axes of the camera and the eye matched each other if the first Purkinje reflex was located in the middle of the pupil. A deviation of the two axes could then be determined by the distance of the Purkinje reflex from the pupillary centre. The required conversion factor was found experimentally both for the horizontal and the vertical direction with the aid of two small spotlights that enclosed an angle of known size with the eye.

To investigate whether a change in refraction with visual angle was caused by astigmatism, we determined the slope of intensity profiles both in the vertical and in the horizontal ocular meridian. For the latter, we rotated the retinoscope by 90° around the optical axis of the camera lens. In the text and in the figures we refer to refractions obtained by the non-rotated retinoscope as the vertical power meridian and to those obtained by the rotated retinoscope as the horizontal power meridian.

### Mapping the ganglion cell density in the retina

In order to evaluate the distribution pattern of the retinal ganglion cells, we labelled them retrogradely with a fluorescent tracer in an *in vitro* preparation. A turtle was decapitated under deep isofluran (Forene; Abbott) anaesthesia. The eyes were dissected from the head. Crystals of tetramethylrhodamine conjugated dextran amine (3,000 MW; Molecular Probes) were applied to the optic nerve stump of the left eye. The preparation was incubated for 48 h at 20°C in a cell culture medium (Dulbecco's MEM/nut mix F-12 HAM; Life Technologies) supplemented with antibiotic and antimycotic substances (4% penicillin-streptomycin and 0.2% amphotericin B; Sigma-Aldrich; see Bellintani-Guardia and Ott 2002 for technical details). Following the incubation period, the anterior portion of the eyeball was carefully cut off at the ora serrata and removed together with the vitreous. The remaining posterior eyecup was fixed overnight in phosphate-buffered saline (PBS, 0.1 mol l<sup>-1</sup>, pH adjusted to 7.4) with 4% paraformaldehyde and then rinsed with PBS. The retina was removed from the sclera and mounted, fibre layer up, as a whole on a glass slide.

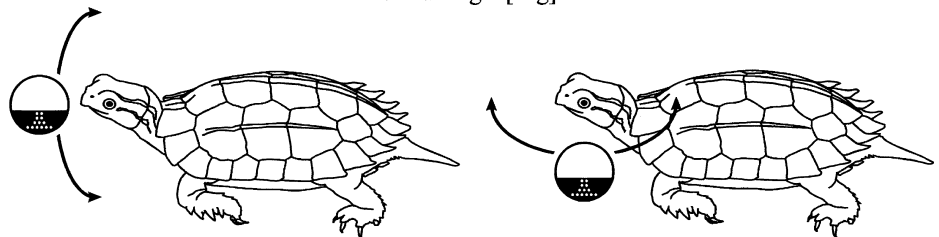
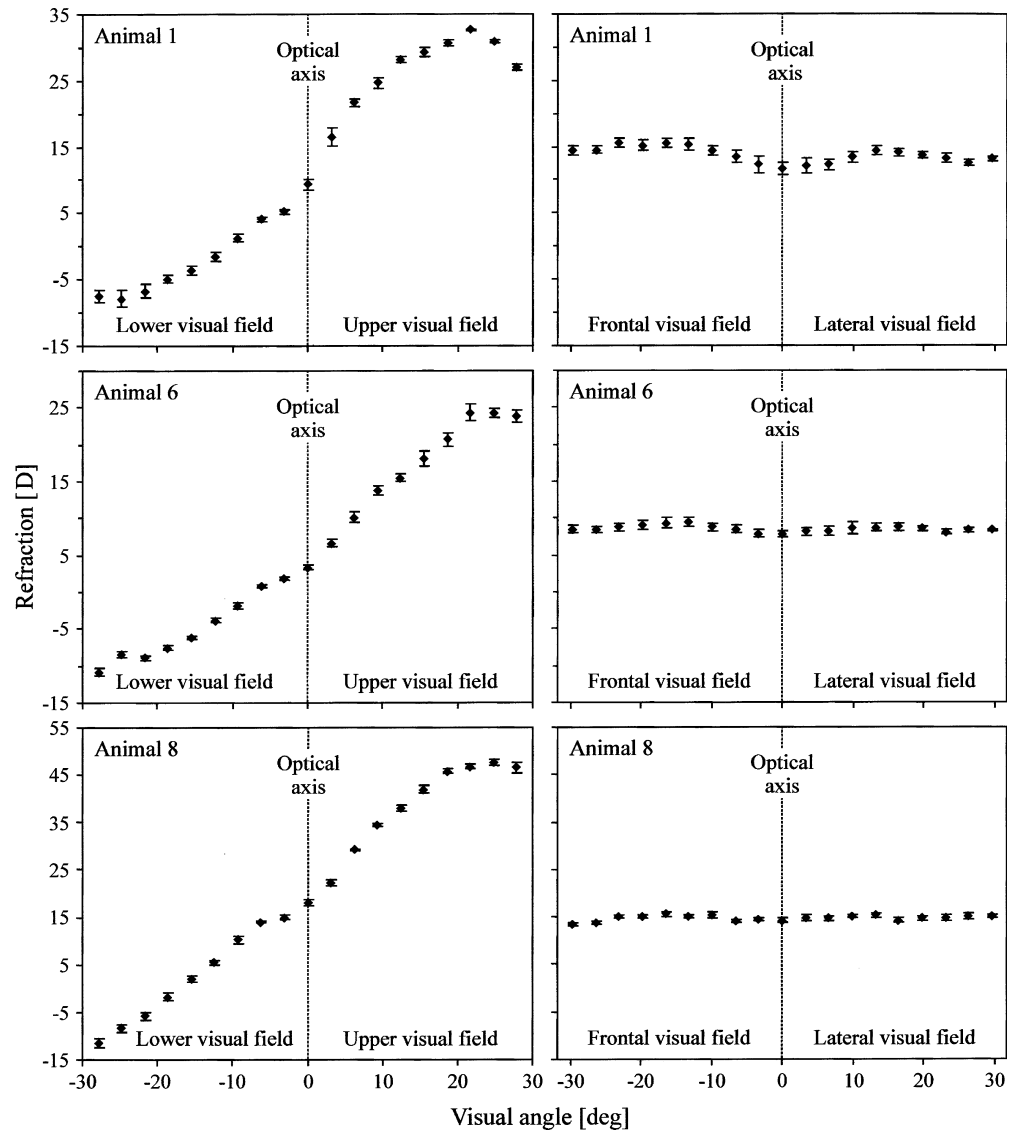
We localized the labelled ganglion cells in the retinal whole-mount with the help of a confocal laser scanning microscope (LSM 410-invert; Zeiss). The fluorophore tetramethylrhodamine was excited by a helium-neon laser (543 nm). Using a 63× objective (water immersion) we examined every 500 μm a square of 135 μm×135 μm. Tangential optical sections of the ganglion cell layer were acquired at steps of 5 μm. This spacing was slightly smaller than the minimal soma diameter of the ganglion cells and excluded that cells were overlooked. A simple computer program allowed us to mark registered somata on the computer screen to avoid multiple counts. The total cell number determined in each patch was then extrapolated to the local cell density per mm<sup>2</sup>.

## Results

### Refractive states across the visual field

In Fig. 2 the refraction of three individuals is plotted against the visual angle for camera turns in the vertical

**Fig. 2** Refractive state across the visual field in three individuals of *G. spengleri*. Refraction of the eye was determined at the optical axis along a vertical (*left column*) and a horizontal (*right column*) plane bisecting the eye. Values were averaged from 7 to 10 camera turns and plotted against the visual angle. In a range  $\pm 30^\circ$  there was no change of the refractive state in the horizontal plane but a marked increase in the vertical plane. The standard deviations (indicated by the *error bars*) were similarly low in all measurements. Note the different scales in the y-axis



(left column) and horizontal (right column) meridian. Data in each diagram originate from the recordings of ten camera turns. The refraction at a certain angle was calculated first by averaging multiple measurements within one turn and finally averaging the corresponding mean values of all turns. Bars represent the standard error (SE). A downward or lateral deviation from the optical axis is indicated by a negative sign, a divergence in an upward or frontal direction by a positive one.

In the horizontal plane, the average refraction and the SE in the frontal and lateral visual field did not differ from values obtained along the optical axis up to angles

of  $30^\circ$ . As an unexpected finding, the measured refraction values were not emmetropic but hyperopic. Values ranged from about 8 to 9 D (animal 6), 12 to 16 D (animal 1) or 13 to 16 D (animal 8) with an SE  $< 1.3$  D. In the vertical plane, the SE were similarly low ( $< 1.4$  D for all angles); the mean refraction, however, decreased continuously from hyperopic values in the upper to myopic values in the lower visual field. The maximum difference observed within  $\pm 30^\circ$  varied considerably in the three animals investigated (35 D for animal 6, 40 D for animal 1 and 59 D for animal 8; note the change in the scale of the ordinates in Fig. 2).

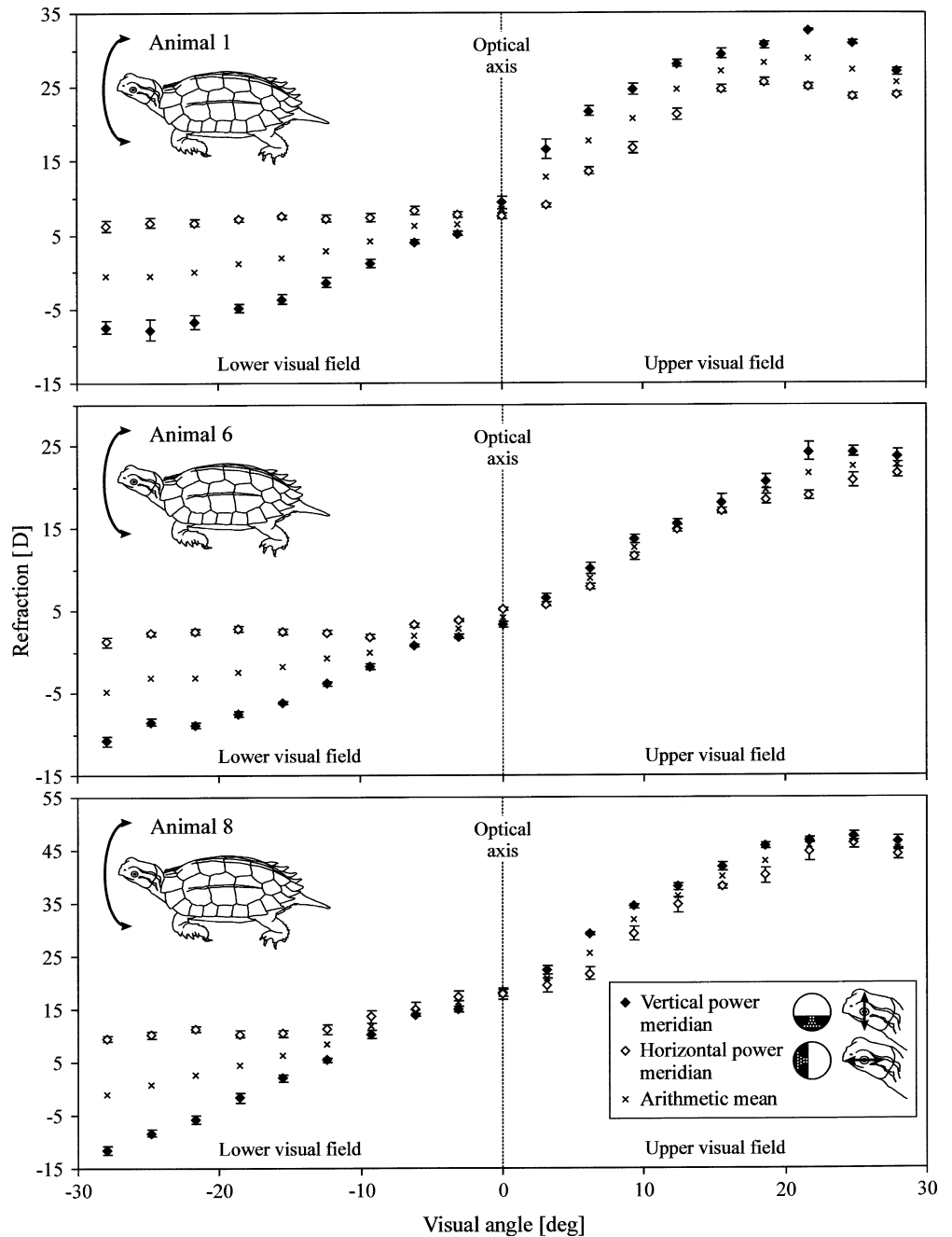
Astigmatism

The experiments illustrated in Fig. 2 were based on measurements in the vertical power meridian of the eye (non-rotated retinoscope). To get more information on the change in the focal state in the upper and lower visual field we determined the refraction also in the horizontal power meridian (retinoscope rotated by 90°) along the vertical circular path of the camera. Data were sampled and averaged as above. They are presented in Fig. 3 (open symbols) together with the corresponding values obtained in the vertical power meridian (solid symbols; already shown in Fig. 2, left column). Fur-

thermore, the arithmetic mean of both values is plotted against the visual angle.

In the upper (dorsal) visual field, refractions measured in the horizontal power meridian displayed a similar increase of hyperopia towards the periphery as in the vertical power meridian. For animals 6 and 8, respectively, the two data sets matched each other quite well, for animal 1 they ran parallel to each other with an average difference of  $6.4 \pm 1.7$  D. In the lower (ventral) visual field, however, all animals displayed an increasing astigmatism from the optical axis to the periphery: Refractions in the vertical power meridian became more and more myopic with respect to the values in the

**Fig. 3** Lower field myopia and astigmatism in three individuals of *G. spengleri*. Refractive state is plotted versus visual angle in the vertical plane bisecting the eye. Refractions in the vertical and horizontal power meridian were averaged from ten camera turns. There was an extensive astigmatism in the lower but not in the upper visual field



horizontal power meridian. The amount of this astigmatism varied remarkably among the three individuals investigated. At  $-28^\circ$  ( $28^\circ$  below the optical axis) the refractive difference between the two meridians amounted to 12 D for animal 6, 14 D for animal 1 and 21 D for animal 8 (note the change in the ordinate scale in Fig. 3). Based on the arithmetic mean of the refractive state in both meridians, we calculated the total change of the refractive state along the vertical plane as 28, 29 and 48 D for animals 6, 1 and 8, respectively. The inter-individual differences disappeared when the astigmatism was considered in proportion to the total change of refractive state from the upper to the lower visual field: in all three animal, the highest refractive difference between the two power meridians was about one-third of the total refractive change of the vertical power meridian in the dorso-ventral plane of the visual field (animal 6:34%; animals 1 and 8:35%).

### Topography of the fundus

Figure 4 shows a large scatter of measured refractive values in the upper visual field (which is projected on the ventral part of the retina) both for the vertical and horizontal power meridian at the position where the optic nerve leaves the bulbus. The pit-like depression of the optic disc resulted in a myopic shift of refraction if it was passed during vertical turns of the camera (open symbols; filled symbols represent camera turns outside the optic disc). In Figs. 2 and 3, the deviations caused by the optic disc were excluded.

**Fig. 4** Topography of the ocular fundus of *G. spengleri*. Refractive state was measured for the vertical (left graph) and horizontal power meridian (right graph) versus visual angle in the vertical plane bisecting the eye. The symbols show refractive values obtained from 2 camera turns. The pit-like depression of the optic disc in the upper visual field is evident both in the vertical and horizontal meridian by a decrease of the refractive values that were represented by open symbols. Filled symbols represent refractive measurements slightly outside the optic disc. Vertical lines superimposed to the symbols represent the range of refractive values obtained from 12 additional camera turns. Values from camera turns that passed through the optic disc were not included in Figs. 2 and 3

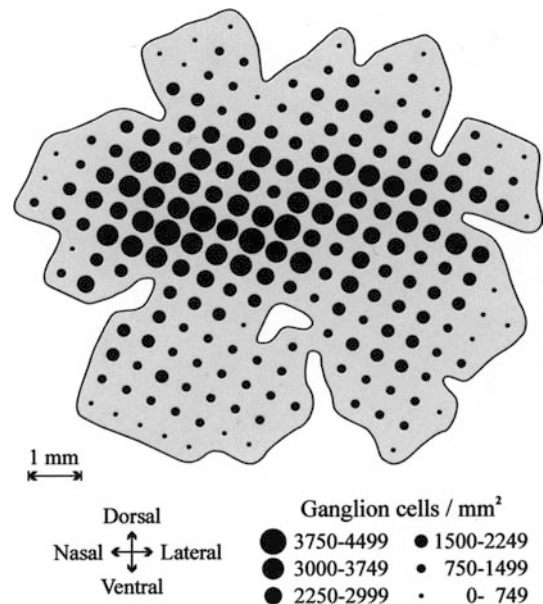
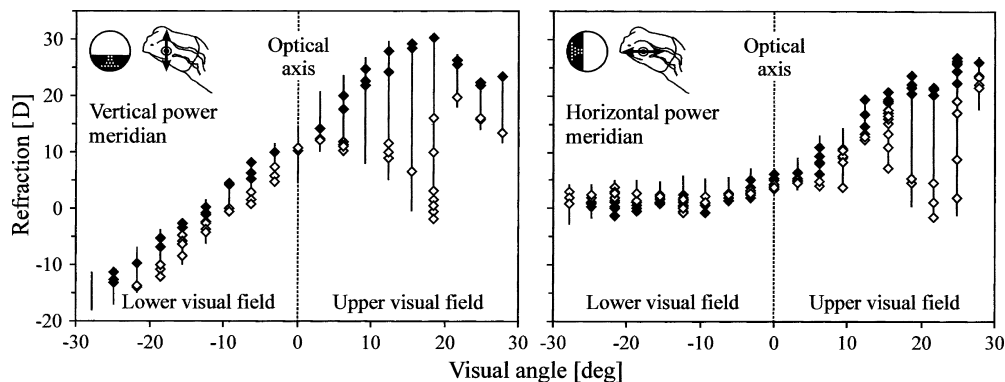


**Fig. 5** Distribution and density of retrogradely labelled ganglion cells in a retina-wholemount of *G. spengleri*. The number of cells  $\text{mm}^{-2}$  was sampled every 500  $\mu\text{m}$  in both  $x$ - and  $y$ -direction and was represented by the size of the dots at the respective locations. The most obvious structural feature is a visual streak, an elongated area of high ganglion cell density, which extends above the optic disc (blank spot in the sketch) from the nasal to the temporal part of the retina. In the centre of this streak, ganglion cell densities reach a maximum of about 4,200 cells  $\text{mm}^{-2}$

### Retinal specializations

Figure 5 shows the number and distribution of retrogradely labelled ganglion cells in a retinal wholemount of *G. spengleri*. The size of the dots in the schematic illustration indicates the local ganglion cell density. The most obvious structural feature in the cell distribution was a visual streak, an elongated area of high cell density which extended above the optic disc from the nasal to the temporal part of the retina. In the centre of this streak, a maximum of about 4,200 ganglion cells  $\text{mm}^{-2}$  was reached. Towards the nasal region, the cell density remained almost as high as in the centre, whereas in the temporal region a somewhat lower density was found. Both times a distinct decline was only found close to the edges. Outside the visual streak, cell density dropped off

distinctly in the ventral part of the retina just below the naso-temporal axis. The decrease in cell density was less pronounced in the dorsal area of the retina, particularly in the naso-dorsal quarter.

## Discussion

In this study, we measured off-axis refractions in the eye of the Vietnamese leaf turtle and compared them to values determined on the optical axis. We made different observations for the two perpendicular planes in the visual field which bisect the eye. Along the horizontal plane, the refractive state did not change and the standard error of the measurements remained equally small at all angles investigated. This showed that the quality of the optical image did not decrease up to  $30^\circ$  off-axis along the horizontal plane bisecting the eye. This, in turn, fits well to the observation of a horizontal visual streak of the retina of *G. spengleri* where a dense package of ganglion cells implied high visual resolution. A horizontal line of enhanced retinal ganglion cell density is not unusual for turtles since it was also found in the retina of several other species (*Pseudemys scripta elegans*: Brown 1969; Peterson and Ulinski 1979; *Caretta caretta*, *Chelonia mydas*, *Dermochelys coriacea*: DeCarlo et al. 1998). Compared to *Pseudemys*, which is commonly used for studies of retinal function, the total density of ganglion cells was unexpectedly lower in *Geoemyda*: The highest cell density in the midpoint of the visual streak exceeded 20,000 cells  $\text{mm}^{-2}$  in *Pseudemys* (Peterson and Ulinski 1979) but only reached about 4,200 cells  $\text{mm}^{-2}$  in *Geoemyda*.

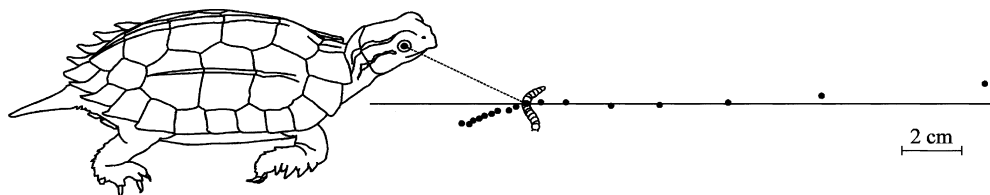
Contrary to expectation, the refractive state of the eye was not emmetropic but hyperopic in all three animals investigated (Fig. 2, right column). This observation could not be attributed to the small eye artefact (Glickstein and Millodot 1970) since this error of the refraction technique was excluded for each turtle by individual calibration. Without direct calibration, a hyperopic offset would be expected since the photoreceptor layer is separated from the reflecting retinal-vit-

reous surface by the thickness of the retina. Since the thickness of the retina is relatively constant in all sizes of eyes (Glickstein and Millodot 1970), this artefact increases with decreasing eye size. In the absence of an object of interest in the darkened laboratory, the animals apparently relaxed their accommodation tonus completely which then led to hyperopia. A hyperopic refractive state was also observed in the resting eye of the chameleon (Ott et al. 1998) and the chicken (F. Schaeffel, unpublished observations).

In the vertical plane of the visual field, the mean refractive state increased continuously from low values in the ventral visual field to higher refractions in the dorsal part. This variation of refractive state was in contrast to the constant values measured in the horizontal field and is best explained as an adaptation to compensate for the different focus distances along the ground plane. Similar observations were obtained from various other vertebrates like birds (Fitzke et al. 1985; Hodos and Erichsen 1990; Schaeffel et al. 1987) and amphibians (Schaeffel et al. 1994). Different to these, we found that the increase of refraction in *G. spengleri* was not confined to the ventral visual field but continued to increase further on in the dorsal visual field. The result was a myopia in the lower visual field and a hyperopia in the upper field.

Strikingly, the strong decrease of the refractive state in the ventral field was not measured in the horizontal power meridian. Although the amount of this astigmatism varied between the individual turtles, it could not be treated as an individual optical aberration since its direction and location in the lower visual field was similar in all three animals. Moreover, the amount of the astigmatism was closely correlated with the total change of the refractive state along the vertical plane irrespective of the inter-individual differences of the refractive state in the vertical power meridian. A similar astigmatism in the ventral visual field was found in the eye of frogs (*Rana*, Schaeffel et al. 1994). While the functional significance of this kind of astigmatism remains unclear both for frogs and leaf turtles it is obvious that it originates from the corneal surface. During our calibrations, we found different locations of the first Purkinje reflex for the same visual angle in the upper and lower visual field. The amount of these differences indicated that the radius of curvature of the cornea decreases from dorsal to ventral. No such difference was found in the naso-temporal direction. A difference of the radius of curvature between the dorso-ventral and naso-temporal direction induces an irregular astigmatism. This, in turn, changes the measured refractive values if the photorefractometer is turned by  $90^\circ$  in accordance to Fig. 3.

**Fig. 6** Adaptive value of the dorso-ventral change of ocular refraction in *G. spengleri*. As the refractive power of the eye decreases steadily from the lower to the upper visual field, the whole ground plane can be kept in focus at a given state of accommodation. This is illustrated in the schematic figure by a turtle that fixates a prey at a distance of 4 cm on the optical axis (broken line). Black spots mark the focal length for different visual angles off-axis. Calculations were based on the arithmetic mean of the refractive state as shown in Fig. 3. It can be seen that all these spots lie approximately on the ground level (horizontal line). The assumed height of the eye above the ground (1.9 cm) was taken from a photograph which was also used as a model for the sketch



As a result of the measured astigmatism, the incoming light rays are not focused to a focal point but, instead, as a horizontal (primary image) and vertical line (secondary image) on two different planes along the optical axis. The best image, the circle of least confusion, lies in between these planes. Accordingly, we calculated the arithmetic mean of both meridians as the actual refractive state in the lower visual field. Figure 6 illustrates the adaptive value of the dorso-ventral change of the refractive state. Various points in focus were calculated along the vertical line of the visual field for a turtle that accommodated on a prey item 4 cm away from the eye. It can be seen that the points in focus were all positioned on a plane corresponding to the ground level. At a given accommodation tonus, this mechanism keeps other objects on the ground also in focus irrespective of their distance to the animal. With the photorefracton technique, it is not possible to distinguish whether the dorso-ventral change in the refractive state is related to differences in the axial length of the eye or to differences in the optical power of the cornea and/or eye lens. In birds, lower field myopia appears to be the result of a changing distance of the plane of photoreceptors with respect to the nodal point of the eye (Land and Nilsson 2002). This is reasonable since the axial growth of the eye is locally controlled for each position in the fundus and influenced by the average viewing distance (Miles and Wallman 1990; Diether and Schaffel 1997).

**Acknowledgements** We thank M. and W. Matzanke for putting their Vietnamese leaf turtles at our disposal to take some preliminary measures. The experiments reported in this paper comply with the *Principles of Animal care*, publication No. 86-23, revised 1985, of the National Institutes of Health and were carried out in accordance with the German "Tierschutzgesetz".

---

## References

- Bellintani-Guardia B, Ott M (2002). Displaced retinal ganglion cells project to the accessory optic system in the chameleon (*Chamaeleo calyptrotus*). *Exp Brain Res* 145:56–63
- Brown KT (1969) A linear area centralis extending across the turtle retina and stabilised to the horizon by non-visual cues. *Vision Res* 9:1053–1062
- Catania AC (1964) On the visual acuity of the homing pigeon. *J Exp Anal Behav* 7:361–366
- DeCarlo L, Salmon M, Wyneken J (1998) Comparative studies of retinal design among sea turtles: histological and behavioral correlates of the visual streak. *Proceedings of the 18th International Symposium on Sea Turtle Biology and Conservation*
- Diether S, Schaeffel F (1997) Local changes in the eye growth induced by imposed local refractive error despite active accommodation. *Vision Res* 37:659–668
- Fitzke FW, Hayes BP, Hodos W, Holden AL, Low JC (1985) Refractive sectors in the visual field of the pigeon eye. *J Physiol (Lond)* 369:17–31
- Glickstein M, Millodot M (1970) Retinoscopy and eye size. *Science* 168:605–606
- Henze M, Schaeffel F, Wagner HJ, Ott M (2004) Accommodation behavior during prey capture in the vietnamese leaf turtle (*Geomyda spengleri*). *J Comp Physiol A* (in press)
- Hodos W, Erichsen T (1990) Lower-field myopia in birds: an adaptation that keeps the ground in focus. *Vision Res* 30:653–657
- Land MF, Nilsson DE (2002) *Animal eyes*. Oxford University Press, New York
- Miles FA, Wallman J (1990) Local ocular compensation for imposed local refractive error. *Vision Res* 30:339–349
- Millodot M, Blough P (1971) The refractive state of the pigeon eye. *Vision Res* 11:1019–1022
- Nye PW (1973) On the functional differences between the frontal and lateral visual fields of the pigeon. *Vision Res* 13:559–574
- Ott M, Schaeffel F, Kirmse W (1998) Binocular vision and accommodation in prey-catching chameleons. *J Comp Physiol A* 182:319–330
- Peterson EH, Ulinski PS (1979) Quantitative studies of retinal ganglion cells in a turtle, *Pseudemys scripta elegans*. I. Number and distribution of ganglion cells. *J Comp Neurol* 186:17–42
- Schaeffel F, Farkas L, Howland HC (1987) Infrared photoretinoscope. *Appl Opt* 26:1505–1509
- Schaeffel F, Hagel G, Eikermann J, Collett T (1994) Lower-field myopia and astigmatism in amphibians and chickens. *J Opt Soc Am A* 11:487–495
- Sivak JG (1976) The accommodative significance of the ramp retina in the eye of the stingray. *Vision Res* 16:945–950
- Walls GL (1942) *The vertebrate eye and its adaptive radiation*. Hafner, New York